Efficient Group-Sparse Transceiver Design for Multiuser MIMO Relaying in C-RAN

Ayoub Saab, Jiaxin Yang, Benoit Champagne and Ioannis Psaromiligkos
Department of Electrical and Computer Engineering, McGill University, Montreal, H3A 0E9, Canada

***Abstract*—This paper addresses the design of multiuser MIMO amplify-and-forward relaying within a cloud radio access network (C-RAN) from an energy-efficiency perspective. The aim is to jointly select remote radio heads and optimize their transceiver in order to assist the communication between multiple source-destination pairs. We formulate the design problem as an interference leakage minimization subject to per-relay power constraints along with linear signal preserving constraints at the destinations. To obtain an energy efficient relaying solution, the objective function is penalized with a regularization term which promotes group-sparsity among the resultant relaying weights. A low-complexity iterative algorithm based on the alternating direction method of multipliers (ADMM) is then proposed to solve the regularized problem. Simulation results demonstrate the explicit benefits of the proposed algorithm, which results in notably lower power consumption and computational complexity than conventional relaying design methods.**

I. Introduction

To meet the increasing demand for high data-rate applications, network densification is prescribed by current cellular communication standards [1]. In this approach, additional access points are deployed in hotspots, creating so-called small cells to support ubiquitous connectivity across the network. To fully exploit the benefits of small-cell networks, advanced interference coordination and resource allocation schemes need to be employed. To enable the low-cost implementation of these sophisticated schemes, a novel centralized radio access network (RAN) architecture, called cloud-RAN (C-RAN), has been proposed for 5G networks [2].

In this new architecture, traditional base station functionalities are apportioned between a centralized baseband unit (BBU) pool and remote radio heads (RRHs). The BBU handles the baseband signal processing functions while the RRHs provide wireless connectivity to the user equipments (UE). Besides reducing the deployment and maintenance costs, C-RAN can improve the network spectral efficiency by exploiting cloud computing to jointly process user data and perform interference coordination. To this end, low-latency and high-bandwidth optical transport links are required to enable the exchange of large amounts of data between the BBU pool and RRHs.The use of powerful BBU, multiple RRHs and high-speed transport links inevitably introduces additional power consumption [3], which has motivated various research efforts devoted to designing energy-efficient (*green*) C-RAN.

Funding for this work was provided by a CRD Grant from the NSERC of Canada, with industrial support from InterDigital Canada.

Energy-efficient transmit solutions for C-RAN have been extensively studied in multi-cell downlink/uplink setups. A group sparse RRH beamforming framework was proposed in [4] with the objective of minimizing the total power consumption in a C-RAN downlink multicast scenario. This approach effectively reduces the number of active RRHs, thus leading to lower network power consumption. The effect of imperfect channel state information (CSI) was addressed in [5] under the same network setup and a robust version of the group sparse beamforming method was proposed. To enhance the group sparsity for downlink multicast beamforming, the smoothed l_p-minimization relying on the iterative reweighted l_2 minimization algorithm was developed in [6]. The joint downlink/uplink network power minimization problem was investigated in [7], where the duality theory was utilized to derive the beamforming solutions. In addition, [8]–[10] addressed the problem of optimizing some alternative network performance metrics under a set of finite-capacity constraints on the transport links.

While most of the prior works focus on coordinated beamforming design in both downlink and uplink setups, the use of RRHs as relays for further improving network coverage and performance, and the associated relay selection and transceiver design algorithms, remain largely unexplored. In [11], the design of a multiuser relaying subnetwork within C-RAN was investigated from an energy-efficient perspective. A joint RRH selection and relay transceiver optimization algorithm was proposed to minimize the network power subject to a set of mean square error-based quality-of-service (QoS) constraints. However, the resultant block-coordinate descent type iterative algorithm exhibits relatively high computational complexity.

In this work, inspired by [11], we investigate the problem of joint relay selection and transceiver optimization in a multiuser amplify-and-forward (AF) relaying subnetwork within C-RAN, but with the additional goal of reducing computational complexity. Specifically, we consider a subnetwork where multiple source-destination pairs communicate with the aid of multiple cooperative RRHs connected to a BBU. In contrast to network power minimization, we formulate the design problem as a regularized sparsity-inducing interference leakage minimization subject to a set of linear signal preserving constraints at the destinations and per-relay power constraints. The problem is then converted into a form that is suitable for the application of the alternating direction method of multipliers (ADMM) [12]. Interestingly, a simple closed-form solution can be derived for each one of the main ADMM

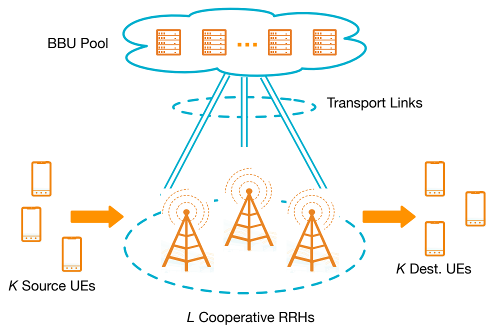

Fig. 1. Multiuser sub-network where communication between the source-destination pairs is assisted by cooperative MIMO relays via the BBU pool.

steps, leading to a very low-complexity iterative algorithm for relay selection and transceiver optimization. Simulation results show that the proposed algorithm can yield a satisfactory QoS level at all destinations with only a subset of active RRHs. In addition, the processing time of the proposed algorithm is significantly reduced as compared to benchmark algorithms relying on external optimization solvers.

The rest of the paper is organized as follows. The C-RAN-based multiuser relaying system model is introduced in Section II. In Section III, the constrained and regularized interference leakage minimization problem is formulated, followed by the development of the low-complexity ADMM-based algorithm. Simulation results are presented and discussed in Section IV. Finally, we conclude the paper in Section V.

II. System Model and Problem Statement

We consider a multiuser relaying sub-network consisting of L RRHs serving as AF relays and K pairs of source and destination UEs, as depicted in Fig. 1. Each source UE is paired with a single destination UE, both modeled as single-antenna nodes due to their limited processing capabilities and low power budgets. By contrast, the l^{th} RRH for $l \in \mathcal{L} = \{1, 2, \dots, L\}$ is equipped with $N_l \geq 1$ antennas. All RRHs are connected to a central node, namely the BBU pool, whose role is to select a proper subset of RRHs and design AF transceiver matrices for these active RRHs. A narrowband flat-fading model is assumed for the radio channels between the UEs and RRHs. The CSI is assumed to be known and remain constant within a given transmission interval. There is no direct link between the source and destination UEs.

Communication is performed in a two-hop half-duplex mode. During the first hop, the k^{th} source UE for $k \in \mathcal{K} = \{1, 2, \dots, K\}$ transmits its information symbol s_k, modeled as a zero-mean complex random variable with variance $\mathrm{E}\left\{|s_k|^2\right\} = p_k$. Let $\mathbf{h}_{lk} \in \mathbb{C}^{N_l \times 1}$ denote the channel vector between the k^{th} source UE and the l^{th} RRH. The latter receives the linear superposition of the transmitted information symbols from each source UE, corrupted by additive noise. This may be expressed as

$$\mathbf{r}_l = \sum_{k=1}^{K} \mathbf{h}_{lk} s_k + \mathbf{n}_l, \tag{1}$$

where $\mathbf{n}_l \in \mathbb{C}^{N_l \times 1}$ is a spatially white noise vector, with zero mean and covariance matrix $\mathbf{\Sigma}_l = \sigma_l^2 \mathbf{I}_{N_l}$. In the AF scheme, the l^{th} RRH applies a linear transformation to $\mathbf{r}_l$, as represented by matrix $\mathbf{B}_l \in \mathbb{C}^{N_l \times N_l}$. The relay transmission power is constrained by an average antenna power budget P_l, i.e.,

$$\operatorname{Tr}\left(\mathbf{B}_l \Big(\sum_{k=1}^{K} p_k \mathbf{h}_{lk} \mathbf{h}_{lk}^H + \sigma_l^2 \mathbf{I}_{N_l} \Big) \mathbf{B}_l{}^H \right) \leq P_l. \tag{2}$$

During the second transmission hop, the k^{th} destination UE receives the sum of the transmitted signals from each RRH along with additive noise, which may be expressed as

$$\begin{aligned} d_k &= \sum_{l=1}^{L} \mathbf{g}_{kl}^H \mathbf{B}_l \mathbf{r}_l + n_k \\ &= S_k + I_k + n_k, \end{aligned} \tag{3}$$

where $\mathbf{g}_{kl}^H \in \mathbb{C}^{1 \times N_l}$ denotes the channel vector between the l^{th} RRH and the k^{th} destination UE, and n_k is the additive noise. The superimposed signals from the RRHs can be expressed as the sum of two distinct components, i.e., the desired signal S_k and the interference leakage I_k:

$$S_k = \sum_{l=1}^{L} \mathbf{g}_{kl}^H \mathbf{B}_l \mathbf{h}_{lk} s_k \tag{4}$$

$$I_k = \sum_{\substack{j=1, \\ j \neq k}}^{K} \sum_{l=1}^{L} \mathbf{g}_{kl}^H \mathbf{B}_l \mathbf{h}_{lj} s_j + \sum_{l=1}^{L} \mathbf{g}_{kl}^H \mathbf{B}_l \mathbf{n}_l. \tag{5}$$

The objective of the relay transceiver optimization is to enhance the reception quality of the desired signal S_k at each destination UE subject to relay power constraints, as specified by (2). Motivated by interference alignment techniques [13], an effective means of achieving this objective is to minimize the *total interference leakage* at all destination UEs, $\sum_{k=1}^{K} \mathrm{E}\{|I_k|^2\}$, while enforcing a set of linear constraints meant to preserve the integrity of the desired signal S_k. Using (4), these constraints can be stated as

$$\sum_{l=1}^{L} \mathbf{g}_{kl}^H \mathbf{B}_l \mathbf{h}_{lk} = c_k, \quad \forall k \in \mathcal{K}, \tag{6}$$

where c_k are predefined positive constants. Hence, the interference leakage minimization problem can be written as

$$\min_{\{\mathbf{B}_l\}_{l \in \mathcal{L}}} \ \mathcal{I} \triangleq \sum_{k=1}^{K} \mathrm{E}\left\{|I_k|^2\right\} \quad \text{s.t. (2) and (6).} \tag{7}$$

In this work, our aim is to solve the above problem, but taking into consideration the energy consumption of the RRHs within the C-RAN framework.

III. Proposed Solution

In this section, we first reformulate (7) in a more compact matrix form, then we incorporate into the formulation a regularization term to encourage the deactivation of a subset of RRHs and thus obtain an energy-efficient solution. Finally, an ADMM-based algorithm is proposed to solve the regularized problem with low complexity.

A. Problem Transformation

We begin by examining the closed-form expression for the total interference leakage in (7) given by

$$\mathcal{I} = \sum_{k=1}^{K} \Big(\sum_{j\neq k} p_j \Big| \sum_{l=1}^{L} \mathbf{g}_{kl}{}^H \mathbf{B}_l \mathbf{h}_{lj} \Big|^2 + \sum_{l=1}^{L} \sigma_l^2 \left\| \mathbf{B}_l^H \mathbf{g}_{kl} \right\|_2^2 \Big). \quad (8)$$

To obtain a more compact expression, we replace each AF matrix by its vectorized version $\mathbf{b}_l = \text{vec}\{\mathbf{B}_l\}$ (obtained by stacking the columns of $\mathbf{B}_l$) and collect the resulting vectors into a global vector $\mathbf{b} \triangleq [\mathbf{b}_1^T, \cdots, \mathbf{b}_L^T]^T$. From the Kronecker product property $\text{vec}(\mathbf{ABC}) = (\mathbf{C}^T \otimes \mathbf{A})\text{vec}(\mathbf{B})$, the first term inside the outer summation in (8) can be expressed as

$$\sum_{j\neq k} p_j \Big| \sum_{l=1}^{L} (\mathbf{h}_{lj}^* \otimes \mathbf{g}_{kl})^H \mathbf{b}_l \Big|^2. \quad (9)$$

Defining $\boldsymbol{\delta}_k^{(j)} \triangleq [(\mathbf{h}_{1j}^* \otimes \mathbf{g}_{k1})^T, (\mathbf{h}_{2j}^* \otimes \mathbf{g}_{k2})^T, \cdots, (\mathbf{h}_{Lj}^* \otimes \mathbf{g}_{kL})^T]^T \in \mathbb{C}^{\sum N_l^2 \times 1}$, we find that the above is equal to

$$\sum_{j\neq k} p_j \Big| \mathbf{b}^H \boldsymbol{\delta}_k^{(j)} \Big|^2 = \mathbf{b}^H \boldsymbol{\Delta}_k \mathbf{b}, \quad (10)$$

with $\boldsymbol{\Delta}_k \triangleq \sum_{j\neq k} p_j \boldsymbol{\delta}_k^{(j)} \boldsymbol{\delta}_k^{(j)H}$. Noting that $\mathbf{I}_{N_l} = \sum_{i=1}^{N_l} \mathbf{e}_i \mathbf{e}_i^H$, where $\mathbf{e}_i$ are the standard basis vectors, the second term in the outer summation in (8) is equal to

$$\sum_{l=1}^{L} \sum_{i=1}^{N_l} \sigma_l^2 \mathbf{g}_{kl}{}^H \mathbf{B}_l \mathbf{e}_i \mathbf{e}_i^H \mathbf{B}_l^H \mathbf{g}_{kl}. \quad (11)$$

Applying the same Kronecker product property as before, we find that (11) is equal to

$$\sum_{l=1}^{L} \mathbf{b}_l^H \mathbf{G}_{kl} \mathbf{b}_l = \mathbf{b}^H \mathbf{G}_k \mathbf{b} \quad (12)$$

with $\mathbf{G}_{kl} \triangleq \sigma_l^2 \sum_{i=1}^{N_l} (\mathbf{e}_i \otimes \mathbf{g}_{kl}) (\mathbf{e}_i \otimes \mathbf{g}_{kl})^H$ and $\mathbf{G}_k = \text{blkdiag}\{\mathbf{G}_{k1}, \mathbf{G}_{k2}, \ldots, \mathbf{G}_{kL}\}$.

Next, we apply the property $\text{Tr}\left(\mathbf{ABA}^H\right) = \text{vec}(\mathbf{A})^H (\mathbf{B} \otimes \mathbf{I}) \,\text{vec}(\mathbf{A})$ to (2) to obtain the following compact formulation

$$\min_{\mathbf{b}} \quad \mathbf{b}^H \boldsymbol{\Theta} \mathbf{b} \quad (13a)$$

$$\text{s.t.} \quad \mathbf{b}_l{}^H \boldsymbol{\Psi}_l \mathbf{b}_l \leq P_l, \quad \forall l \in \mathcal{L} \quad (13b)$$

$$\boldsymbol{\Phi}^H \mathbf{b} = \mathbf{c}, \quad (13c)$$

where we define

$$\boldsymbol{\Theta} \triangleq \sum_{k=1}^{K} (\boldsymbol{\Delta}_k + \mathbf{G}_k), \quad (14)$$

$$\boldsymbol{\Psi}_l \triangleq \Big(\sum_{k=1}^{K} p_k \mathbf{h}_{lk} \mathbf{h}_{lk}^H + \boldsymbol{\Sigma}_l \Big) \otimes \mathbf{I}_{N_l}, \quad (15)$$

$\mathbf{c} \triangleq [c_1, c_2, \cdots, c_K]^T$ and $\boldsymbol{\Phi} \triangleq [\boldsymbol{\phi}_{l,k}] \in \mathbb{C}^{\sum_{l=1}^{L} N_l^2 \times K}$, which is partitioned into $L \times K$ blocks, each given by $\boldsymbol{\phi}_{l,k} = \mathbf{h}_{lk}^* \otimes \mathbf{g}_{kl}$.

We emphasize that at this stage of the formulation, nothing prevents any of the RRHs from participating in the relay-assisted transmission, potentially leading to a situation where all RRHs are activated. In the following, we modify (13) by adding a regularization term to reduce the number of active RRHs while still providing an acceptable QoS level.

B. Relay Selection via Group-Sparsity

We first note that the l^{th} RRH being inactive is equivalent to $\|\mathbf{b}_l\|_2 = 0$. Consequently, having a small set of active RRHs implies that the solution vector $\mathbf{b}$ is characterized by the so-called group-sparsity [4], that is, $\mathcal{B} \triangleq \left[\|\mathbf{b}_1\|_2, \cdots, \|\mathbf{b}_L\|_2\right]^T$ consists of a reduced number of non-zero elements. This property can be captured by the l_0-norm $\|\mathcal{B}\|_0$.

Bearing in mind that our ultimate goal is to design an energy efficient solution, a group-sparse solution is desired. Motivated by the widely used least absolute shrinkage and selection operator (LASSO) method in the machine learning literature [14], an efficient way to promote the group sparsity during the optimization is to penalize the objective function (13a) with an l_1-norm term on $\mathcal{B}$, $\|\mathcal{B}\|_1 = \sum_{l=1}^{L} \|\mathbf{b}_l\|_2$. We may penalize the objective function (13) by the regularization term $\sum_{l=1}^{L} \lambda_l \|\mathbf{b}_l\|_2$ with $\lambda_l > 0$ being an adjustable parameter representing the weight given to the l^{th} RRH.

To further simplify the presentation, we define $\boldsymbol{\Psi} \triangleq \text{blkdiag}\{\boldsymbol{\Psi}_1, \cdots, \boldsymbol{\Psi}_L\}$ and $\mathbf{x} \triangleq \boldsymbol{\Psi}^{1/2}\mathbf{b} = [\mathbf{x}_1^T, \cdots, \mathbf{x}_L^T]^T$ with $\mathbf{x}_l = \boldsymbol{\Psi}_l^{1/2} \mathbf{b}_l$. Note that the sample covariance matrix $\boldsymbol{\Psi}_l$ in (15) is non-singular, which implies that whether $\|\mathbf{x}_l\|_2 > 0$ or $\|\mathbf{x}_l\|_2 = 0$ depends entirely on whether $\|\mathbf{b}_l\|_2 > 0$ or $\|\mathbf{b}_l\|_2 = 0$. Hence, both vectors $\mathbf{x}$ and $\mathbf{b}$ share the same group-sparsity structure. Based on this observation, a regularized version of (13) can be given by

$$\min_{\mathbf{x}} \quad \mathbf{x}^H \breve{\boldsymbol{\Theta}} \mathbf{x} + \sum_{l=1}^{L} \lambda_l \|\mathbf{x}_l\|_2 \quad (16a)$$

$$\text{s.t.} \quad \mathbf{x}_l^H \mathbf{x}_l \leq P_l, \quad \forall l \in \mathcal{L} \quad (16b)$$

$$\breve{\boldsymbol{\Phi}}^H \mathbf{x} = \mathbf{c}, \quad (16c)$$

where $\breve{\boldsymbol{\Theta}} \triangleq \boldsymbol{\Psi}^{-\frac{1}{2}} \boldsymbol{\Theta} \boldsymbol{\Psi}^{-\frac{1}{2}}$ and $\breve{\boldsymbol{\Phi}} \triangleq \boldsymbol{\Psi}^{-\frac{1}{2}} \boldsymbol{\Phi}$.

It can be seen that the above problem is convex, and therefore can be solved with global optimality using a standard optimization package via the interior point method [15].

C. ADMM-based Low-Complexity Algorithm

In what follows, we develop an algorithm for solving the regularized relaying optimization problem (16) based on ADMM [12]. In particular, we show that each step of the ADMM admits a closed-form solution, which can significantly reduce the computational complexity of the algorithm.

To rewrite (16) in a form amenable to the ADMM, we introduce a synthesized copy of $\mathbf{x}$, namely $\mathbf{z}$, via the linear constraint $\mathbf{x} = \mathbf{z}$. Introducing the constraint sets

$$\mathcal{C}_1 : \breve{\boldsymbol{\Phi}}^H \mathbf{x} = \mathbf{c} \quad (17)$$

$$\mathcal{C}_2 : \mathbf{z}_l^H \mathbf{z}_l \leq P_l, \quad \forall l \in \mathcal{L}, \quad (18)$$

(16) can be re-expressed as

$$\min_{\mathbf{x},\mathbf{z}} \ \mathbf{x}^H \breve{\mathbf{\Theta}} \mathbf{x} + \sum_{l=1}^{L} \lambda_l \|\mathbf{z}_l\|_2 \tag{19a}$$

$$\text{s.t.} \ \ \mathbf{x} \in \mathcal{C}_1, \ \ \mathbf{z} \in \mathcal{C}_2, \ \ \mathbf{x} = \mathbf{z}. \tag{19b}$$

The ADMM algorithm aims to iteratively minimize the augmented Lagrangian given by

$$\begin{aligned}\mathcal{L}_\rho(\mathbf{x},\mathbf{z},\mathbf{y}) = \mathbf{x}^H \breve{\mathbf{\Theta}} \mathbf{x} + \frac{\rho}{2}\|\mathbf{z}-\mathbf{x}\|_2^2 + \sum_{l=1}^{L} \lambda_l \|\mathbf{z}_l\|_2 \\ - (\mathbf{z}-\mathbf{x})^H \mathbf{y} - \mathbf{y}^H(\mathbf{z}-\mathbf{x}),\end{aligned} \tag{20}$$

where $\rho > 0$ is an algorithm parameter, which is assumed to remain constant during the ADMM iterations, and $\mathbf{y}$ denotes the Lagrange multiplier associated with the constraint $\mathbf{x} = \mathbf{z}$. We note that an optimal solution $(\mathbf{x}^{\text{opt}}, \mathbf{z}^{\text{opt}}, \mathbf{y}^{\text{opt}})$ that minimizes $\mathcal{L}_\rho(\mathbf{x},\mathbf{z},\mathbf{y})$ must satisfy $\mathbf{x}^{\text{opt}} = \mathbf{z}^{\text{opt}}$ since $\mathbf{z}$ is a synthesized copy of $\mathbf{x}$. Therefore, solving (19) becomes equivalent to solving the following problem,

$$\min_{\mathbf{x},\mathbf{z}} \ \mathcal{L}_\rho(\mathbf{x},\mathbf{z},\mathbf{y}) \tag{21a}$$

$$\text{s.t.} \ \ \mathbf{x} \in \mathcal{C}_1, \ \ \mathbf{z} \in \mathcal{C}_2, \ \ \mathbf{x} = \mathbf{z}. \tag{21b}$$

The basic idea behind ADMM is to solve the above problem with respect to $\mathbf{x}$ and $\mathbf{z}$ separately in an alternating manner, i.e., one variable at a time with the other fixed. After each round of update of $\mathbf{x}$ and $\mathbf{z}$, the dual variable $\mathbf{y}$ is updated to ensure that $\mathbf{x}$ and $\mathbf{z}$ become closer to each other. In effect, the above optimization problem can now be decoupled into three separate steps, all of which, interestingly, admit a simple closed-form solution, as detailed below.

1) Update $\mathbf{x}$*:* The subproblem solving for $\mathbf{x}$ can be expressed as $\min_{\mathbf{x}\in\mathcal{C}_1} \mathcal{L}_\rho(\mathbf{x},\mathbf{z},\mathbf{y})$, with $\mathbf{z}$ and $\mathbf{y}$ fixed. Using (20), the above subproblem can further be expressed as the following linearly-constrained quadratic program after neglecting all terms that are independent of $\mathbf{x}$:

$$\mathbf{x}^{\text{opt}} = \arg\min_{\mathbf{x}} \ \mathbf{x}^H \breve{\mathbf{\Theta}} \mathbf{x} + \frac{\rho}{2}\|\mathbf{z}-\mathbf{x}\|_2^2 + \mathbf{y}^H\mathbf{x} + \mathbf{x}^H\mathbf{y} \tag{22a}$$

$$\text{s.t.} \quad \breve{\mathbf{\Phi}}^H \mathbf{x} = \mathbf{c}. \tag{22b}$$

It is observed that the objective function (22a) is strictly convex in $\mathbf{x}$ and Slater's constraint qualification holds, i.e., (22) is strictly feasible. Hence, the Karush-Khun-Tucker sufficient conditions hold for the optimal solution $\mathbf{x}^{\text{opt}}$ together with some optimal dual variable $\boldsymbol{\nu}^{\text{opt}}$, yielding:

$$\begin{cases} \mathbf{Q}\,\mathbf{x}^{\text{opt}} = \frac{\rho}{2}\mathbf{z} - \mathbf{y} + \breve{\mathbf{\Phi}}\boldsymbol{\nu}^{\text{opt}} \\ \breve{\mathbf{\Phi}}^H \mathbf{x}^{\text{opt}} = \mathbf{c} \end{cases}, \tag{23}$$

where $\mathbf{Q} \triangleq \breve{\mathbf{\Theta}} + \frac{\rho}{2}\mathbf{I}_{\sum N_l^2}$.

Re-arranging the first equation in (23), we obtain

$$\mathbf{x}^{\text{opt}} = \mathbf{Q}^{-1}\left(\frac{\rho}{2}\mathbf{z} - \mathbf{y} + \breve{\mathbf{\Phi}}\boldsymbol{\nu}^{\text{opt}}\right). \tag{24}$$

To determine the value of the optimal dual variable $\boldsymbol{\nu}^{\text{opt}}$, we substitute (24) back into the second equation of (23). After some matrix manipulations, $\boldsymbol{\nu}^{\text{opt}}$ is given by

$$\boldsymbol{\nu}^{\text{opt}} = \breve{\mathbf{Q}}^{-1}\left(\mathbf{c} - \breve{\mathbf{\Phi}}^H \mathbf{Q}^{-1}(\frac{\rho}{2}\mathbf{z} - \mathbf{y})\right), \tag{25}$$

where $\breve{\mathbf{Q}} \triangleq \breve{\mathbf{\Phi}}^H \mathbf{Q}^{-1} \breve{\mathbf{\Phi}}$. Then substituting (25) back into (24), the following closed-form solution is obtained

$$\mathbf{x}^{\text{opt}} = \mathbf{Q}^{-1}\Big(\big(\mathbf{I} - \breve{\mathbf{\Phi}}\breve{\mathbf{Q}}^{-1}\breve{\mathbf{\Phi}}^H\mathbf{Q}^{-1}\big)\big(\frac{\rho}{2}\mathbf{z} - \mathbf{y}\big) + \breve{\mathbf{\Phi}}\breve{\mathbf{Q}}^{-1}\mathbf{c}\Big). \tag{26}$$

2) Update $\mathbf{z}$*:* Similarly, the subproblem solving for $\mathbf{z}$ can be written as $\min_{\mathbf{z}\in\mathcal{C}_2} \mathcal{L}_p(\mathbf{x},\mathbf{z},\mathbf{y})$, where the values $\mathbf{x}$ and $\mathbf{y}$ are obtained from the previous iteration. Observing that the first term in (20) is independent of $\mathbf{z}$, we write

$$\mathbf{z}^{\text{opt}} = \arg\min_{\mathbf{z}\in\mathcal{C}_2} \sum_{l=1}^{L} \lambda_l \|\mathbf{z}_l\|_2 + \frac{\rho}{2}\|\mathbf{z}-\mathbf{x}\|_2^2 - \mathbf{y}^H\mathbf{z} - \mathbf{z}^H\mathbf{y}. \tag{27}$$

Decoupling (27) over each $\mathbf{z}_l$, we obtain L parallel subproblems each expressed by

$$\mathbf{z}_l^{\text{opt}} = \arg\min_{\|\mathbf{z}_l\|_2^2 \le P_l} \lambda_l \|\mathbf{z}_l\|_2 + \frac{\rho}{2}\|\mathbf{z}_l - \mathbf{x}_l\|_2^2 - \mathbf{y}_l^H \mathbf{z}_l - \mathbf{z}_l^H \mathbf{y}_l, \tag{28}$$

where the original Lagrange multiplier may be decomposed into L such multipliers, i.e., $\mathbf{y} = [\mathbf{y}_1^T, \mathbf{y}_2^T, \ldots, \mathbf{y}_L^T]^T$. To find a closed-form solution, we first present the following lemma, whose proof is omitted due to lack of space.

Lemma 1: Consider the convex minimization problem

$$\min_{\|\mathbf{x}\|_2^2 \le P} \lambda\|\mathbf{x}\|_2 + \frac{\rho}{2}\mathbf{x}^H\mathbf{x} - \mathbf{x}^H\mathbf{a} - \mathbf{a}^H\mathbf{x}. \tag{29}$$

The global minimizer $\mathbf{x}^{\text{opt}}$ admits the closed-form solution

$$\mathbf{x}^{\text{opt}} = \frac{\mathbf{a}}{\|\mathbf{a}\|_2\left(\frac{\rho}{2} + \eta^{\text{opt}}\right)}[\|\mathbf{a}\|_2 - \lambda]_+ \tag{30}$$

where $[c]_+ \triangleq \max\{0, c\}$ and the optimal dual variable η^{opt} associated with the quadratic constraint $\|\mathbf{x}\|_2^2 \le P$ is given by

$$\eta^{\text{opt}} = \left[\frac{[\|\mathbf{a}\|_2 - \lambda]_+}{\sqrt{P}} - \frac{\rho}{2}\right]_+. \tag{31}$$

□

Using Lemma 1, the optimal solution to (28) is given by

$$\mathbf{z}_l^{\text{opt}} = \frac{\mathbf{a}_l}{\|\mathbf{a}_l\|_2\left(\frac{\rho}{2} + \eta_l\right)}[\|\mathbf{a}_l\|_2 - \lambda_l]_+ \tag{32}$$

where $\eta_l = \left[\frac{\|\mathbf{a}_l\|_2 - \lambda_l}{\sqrt{P_l}} - \frac{\rho}{2}\right]_+$ and $\mathbf{a}_l = \frac{\rho}{2}\mathbf{x}_l + \mathbf{y}_l$.

In summary, both the updates of $\mathbf{x}$ and $\mathbf{z}$ are obtained in closed-form at each iteration with the aid of (26) and (32). In addition, the update step for $\mathbf{z}$ can be carried out in a parallel fashion. The ADMM-based algorithm is now summarized in Algorithm 1, where the primal and dual residuals are defined as follows (see [12]),

$$\mathbf{r}^{(j+1)} = \mathbf{x}^{(j+1)} - \mathbf{z}^{(j+1)}, \tag{33}$$

$$\mathbf{s}^{(j+1)} = -\frac{\rho}{2}(\mathbf{z}^{(j+1)} - \mathbf{z}^{(j)}), \tag{34}$$

and $\epsilon_r, \epsilon_s > 0$ denote the tolerance parameters.

Algorithm 1 ADMM for solving (16)

Initialization: primal variable $\mathbf{z}^{(0)}$ (arbitrary non-zero vector); dual variable $\mathbf{y}^{(0)} = \mathbf{0}$; set ADMM iteration index $j = 0$;

repeat

  Update $\mathbf{x}^{(j+1)}$ using (26)

  Update $\mathbf{z}_l^{(j+1)}$ using (32) for all $l \in \mathcal{L}$.

  Update the Lagrange multiplier $\mathbf{y}$ by

$$\mathbf{y}^{(j+1)} = \mathbf{y}^{(j)} + \frac{\rho}{2}\left(\mathbf{x}^{(j+1)} - \mathbf{z}^{(j+1)}\right)$$

  $j \leftarrow j + 1$;

until $\|\mathbf{r}^{(j+1)}\|_2 \le \epsilon_r$ and $\|\mathbf{s}^{(j+1)}\|_2 \le \epsilon_s$

D. An Improved Two-Stage ADMM Implementation

The ADMM-based algorithm is capable of selecting a subset of active RRHs. However, similar to the LASSO problem in compressive sensing literature, the addition of the norm-based regularization term in the objective function [c.f. (16a)] may lead to worse relaying performance, which can be improved by solving for the optimal relaying AF matrices one more time for those active RRHs selected from the previous step. This problem can be formulated as

$$\min_{\breve{\mathbf{x}}} \quad \breve{\mathbf{x}}^H \breve{\mathbf{\Theta}}_{\mathrm{R}} \breve{\mathbf{x}} \tag{35a}$$

$$\text{s.t.} \quad \mathbf{x}_l^H \mathbf{x}_l \le P_l, \quad \forall l \in \mathcal{A} \tag{35b}$$

$$\breve{\mathbf{\Phi}}_{\mathrm{R}}^H \breve{\mathbf{x}} = \mathbf{c}, \tag{35c}$$

where $\breve{\mathbf{x}}$ now only consists of weights from active RRHs and $\mathcal{A} \triangleq \{l \in \mathcal{L} : \|\mathbf{z}_l\|_2 > 0\}$ denotes the subset of active RRHs. Note that $\breve{\mathbf{\Theta}}_{\mathrm{R}}$ and $\breve{\mathbf{\Phi}}_{\mathrm{R}}$ are reduced versions of $\mathbf{\Theta}$ and $\mathbf{\Phi}$, where elements related to the inactive RRHs are deleted. The two-stage ADMM implementation is now summarized as follows:

1) Solve (16) using Algorithm 1 and determine the subset of active RRHs $\mathcal{A}$;
2) Solve (35) for active RRHs using ADMM[1].

IV. Results and Discussion

In all our simulations, we consider a relaying sub-network consisting of $K = 6$ source-destination pairs and $L = 6$ RRHs. For simplicity, we use the same number of antennas and power budget for all RRHs, i.e., $N_l = 4$ and $P_l = 2W$ for all l. The channel coefficients are generated as independent and identically distributed zero-mean complex circular Gaussian variables with unit variance. The noise variances at the RRHs, σ_l^2, are set according to the desired input relay signal-to-noise ratios (SNR), defined as $\gamma_l = \frac{P_l}{N_l \sigma_l^2}$. All the simulation results are averaged over 100 independent realizations.

Fig. 2 shows the convergence behavior of Algorithm 1 for one specific channel realization. It can be observed from the top-left figure that the value of the objective function, i.e. (16a), monotonically decreases with the iteration number. In

[1]The development of an ADMM-based solution for this simplified problem parallels that in Section III and is omitted due to space limitations.

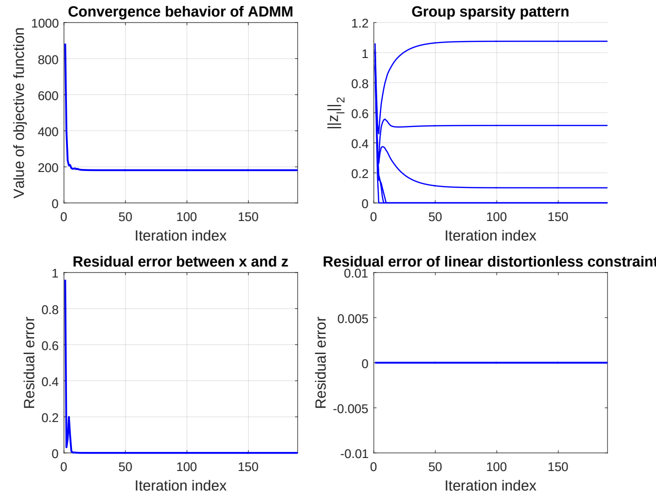

Fig. 2. Convergence behavior of the proposed ADMM-based algorithm with $\gamma_l = 15$ dB, $\lambda = 100$ and $\epsilon_r = \epsilon_s = 10^{-5}$.

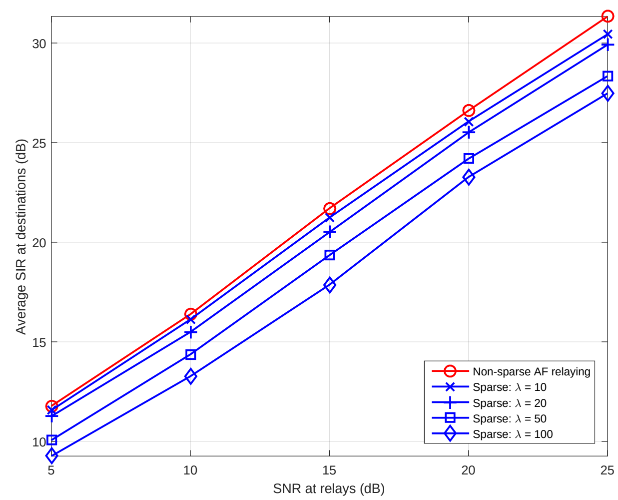

Fig. 3. Achievable average SIR at all destination versus the relay input SNR

the top-right figure, it is observed that the norm of relaying weights, i.e. $\|\mathbf{z}_l\|_2$, for three RRHs approaches zero. In effect, this means that for this specific realization, the algorithm yields a subset of three active RRHs.

In Fig. 3, we evaluate the achieved average signal-to-interference ratio (SIR) at all destinations (defined as $\frac{1}{K}\sum_{k=1}^{K}(\mathrm{E}\{|S_k|^2\}/\,\mathrm{E}\{|I_k|^2\})$, c.f. [(4), (5)]) as a function of the relay input SNR. We vary the regularization parameter λ to examine the tradeoff between the achievable network performance and the energy efficiency in terms of the number of active relays and the total network energy consumption. It is shown that the non-sparse relay beamforming solution, which solves (16) without the regularization term, i.e., $\lambda = 0$, yields the best received SIR as expected since all the RRHs are involved in the transmission. As the value of λ increases, a gap

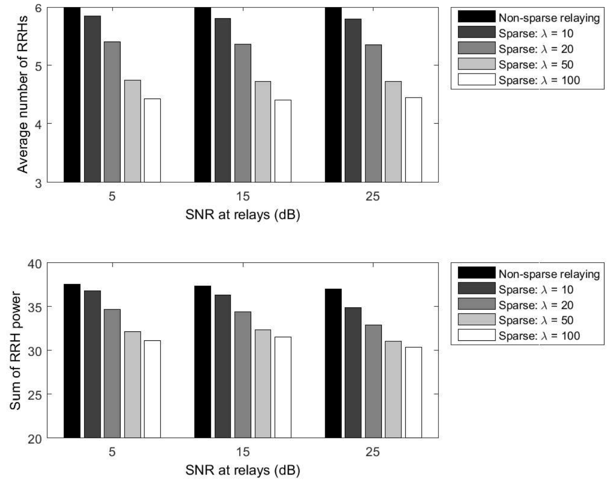

Fig. 4. Top figure: average number of active RRHs versus the regularization parameter λ. Bottom figure: sum of RRH power versus the regularization parameter λ. The front-haul power is set to $P_{c,l} = 5.6W$ for all RRHs [6].

between the performance of the non-sparse solution and the proposed group-sparse solution can be observed. For instance, at the relay input SNR level of 15dB, selecting $\lambda = 50$ leads to a reduction in the achieved SIR of around 3dB.

To gain more intuition behind the performance reduction observed in Fig. 3, we show the average number of active RRHs and their total power consumption with varying λ in Fig. 4. It is observed that for all relay input SNR levels, on average less than 5.5 RRHs are active for the case of $\lambda = 20$ while less than 4.5 RRHs are active for the case of $\lambda = 100$. The RRH individual power is defined as $P_l = \frac{1}{\eta_l} P_{t,l} + P_{c,l}$, where η_l denotes the efficiency of the power amplifier, e.g., $\eta_l = 50\%$ [16], $P_{t,l}$ denotes the RRH transmission power ([c.f., (2)]) and $P_{c,l}$ denotes the front-haul link power consumption [6], which can be saved when the lth RRH is switched off. The proposed group-sparse yields a 17% reduction in the sum RRH power. Based on the results, it becomes evident that the proposed solution can improve the network energy efficiency while still providing a satisfactory level of QoS for all the end-users.

Finally, we compare the processing time of the proposed algorithm with two methods relying on external optimization solvers, specifically, `SeDuMi` and `MOSEK`. The external solver-based approaches solve (16) and (35) by directly invoking the corresponding solvers. The results, listed in Table I, show that the complexity of the proposed algorithm represents only a small fraction of that of the solver-based solutions.

TABLE I
PROCESSING TIME OF DIFFERENT SOLUTIONS (IN SECONDS)

	Regularization parameter λ				
	1	10	20	50	100
SeDuMi	0.1658	0.2992	0.2293	0.2367	0.2391
MOSEK	0.0349	0.0459	0.0473	0.0506	0.0509
Proposed	0.0056	0.0077	0.0098	0.0118	0.0130

V. CONCLUSIONS

A low-complexity joint RRH selection and relay AF transceiver optimization algorithm was proposed for a multiuser relaying network within a C-RAN. The design problem was formulated to minimize the total interference received at all destinations subject to a set of linear signal preservation constraints and per-relay power constraints. A regularization term representing the group sparsity pattern associated with the relay AF matrices was added to the objective function. A two-stage ADMM-based algorithm was then proposed to solve the design problem. Simulation results show that the proposed algorithm leads to lower power consumption and computational complexity than conventional relaying methods.

REFERENCES

[1] 3GPP TR 36.872, "3rd generation partnership project; technical report (tr); Small cell enhancements for E-UTRA and E-UTRAN - Physical layer aspects (Release 12)," 2013.

[2] A. Checko, H. L. Christiansen, Y. Yan, L. Scolari, G. Kardaras, M. S. Berger, and L. Dittmann, "Cloud RAN for mobile networks – A technology overview," *IEEE Commun. Surveys Tuts.*, vol. 17, no. 1, pp. 405–426, 1st qtr. 2015.

[3] *C-RAN White Paper: The Road Towards Green RAN*, Dec. 2013. [Online]. Available: http://labs.chinamobile.com/cran

[4] Y. Shi, J. Zhang, and K. B. Letaief, "Group sparse beamforming for green cloud-RAN," *IEEE Trans. Wireless Commun.*, vol. 13, no. 5, pp. 2809–2823, May 2014.

[5] ——, "Robust group sparse beamforming for multicast green cloud-RAN with imperfect CSI," *IEEE Trans. Signal Process.*, vol. 63, no. 17, pp. 4647–4659, Sept 2015.

[6] Y. Shi, J. Cheng, J. Zhang, B. Bai, W. Chen, and K. B. Letaief, "Smoothed l_p-minimization for green cloud-RAN with user admission control," *IEEE J. Sel. Areas Commun.*, vol. 34, no. 4, pp. 1022–1036, Apr. 2016.

[7] S. Luo, R. Zhang, and T. J. Lim, "Downlink and uplink energy minimization through user association and beamforming in C-RAN," *IEEE Trans. Wireless Commun.*, vol. 14, no. 1, pp. 494–508, Jan 2015.

[8] B. Dai and W. Yu, "Sparse beamforming and user-centric clustering for downlink cloud radio access network," *IEEE Access*, vol. 2, pp. 1326–1339, 2014.

[9] L. Liang and Z. Rui, "Downlink SINR balancing in C-RAN under limited fronthaul capacity," in *Proc. IEEE Int. Conf. Acoust., Speech Signal Process. (ICASSP)*, Mar 2016, pp. 3506–3510.

[10] V. N. Ha and L. B. Le, "Joint coordinated beamforming and admission control for fronthaul constrained cloud-rans," in *Proc. IEEE Global Commun. Conf. (Globecom)*, Dec 2014, pp. 4054–4059.

[11] J. Yang, B. Champagne, Y. Zou, and L. Hanzo, "Centralized energy-efficient multiuser multiantenna relaying in next-generation radio access networks," *IEEE Trans. Veh. Technol.*, vol. 66, no. 9, pp. 7913–7924, Sept 2017.

[12] S. Boyd, N. Parikh, E. Chu, B. Peleato, and J. Eckstein, "Distributed optimization and statistical learning via the alternating direction method of multipliers," *Found. Trends Mach. Learn.*, vol. 3, no. 1, pp. 1–122, Jan. 2011. [Online]. Available: http://dx.doi.org/10.1561/2200000016

[13] P. Mohapatra, K. E. Nissar, and C. R. Murthy, "Interference alignment algorithms for the K user constant MIMO interference channel," *IEEE Trans. on Signal Processing*, vol. 59, no. 11, pp. 5499–5508, nov 2011.

[14] M. Yuan and Y. Lin, "Model selection and estimation in regression with grouped variables," *Journal of the Royal Statistical Society: Series B (Statistical Methodology)*, vol. 68, no. 1, pp. 49–67, 2006.

[15] S. Boyd and L. Vandenberghe, *Convex Optimization*. Cambridge University Press, 2004.

[16] Feb. 2013. [Online]. Available: http://global-sei.com/news/press/13/prs012_s.html